



HAL
open science

Lyotropic Liquid-Crystalline Phases of Sophorolipid Biosurfactants

Fella Saci, Sophie L K W Roelants, Wim Soetaert, Niki Baccile, Patrick Davidson

► **To cite this version:**

Fella Saci, Sophie L K W Roelants, Wim Soetaert, Niki Baccile, Patrick Davidson. Lyotropic Liquid-Crystalline Phases of Sophorolipid Biosurfactants. 2022. hal-03865832v1

HAL Id: hal-03865832

<https://hal.science/hal-03865832v1>

Preprint submitted on 30 Jun 2022 (v1), last revised 3 Jan 2023 (v2)

HAL is a multi-disciplinary open access archive for the deposit and dissemination of scientific research documents, whether they are published or not. The documents may come from teaching and research institutions in France or abroad, or from public or private research centers.

L'archive ouverte pluridisciplinaire **HAL**, est destinée au dépôt et à la diffusion de documents scientifiques de niveau recherche, publiés ou non, émanant des établissements d'enseignement et de recherche français ou étrangers, des laboratoires publics ou privés.

Lyotropic Liquid-Crystalline Phases of Sophorolipid Biosurfactants

Fella Saci,^a Sophie L. K. W. Roelants,^{b,c} Wim Soetaert,^{b,c} Niki Baccile,^{a} Patrick Davidson^{d*}*

^a Sorbonne Université, Centre National de la Recherche Scientifique, Laboratoire de Chimie de la Matière Condensée de Paris, LCMCP, F-75005 Paris, France

^b Centre for Industrial Biotechnology and Biocatalysis (InBio.be), Department of Biotechnology, Faculty of Bioscience Engineering, Ghent University, Coupure Links 653, 9000 Ghent, Belgium

^c Bio Base Europe Pilot Plant, Rodenhuisenkaai 1, 9042 Ghent, Belgium

^d Laboratoire de Physique des Solides, Université Paris-Saclay, Centre National de la Recherche Scientifique, 91405 Orsay, France.

* Corresponding authors:

Dr. Patrick Davidson

patrick.davidson@universite-paris-saclay.fr

Dr. Niki Baccile

niki.baccile@sorbonne-universite.fr

ABSTRACT: Biological amphiphiles derived from natural resources are presently being investigated in the hope that they will someday replace current synthetic surfactants, which are known pollutants of soils and water resources. Sophorolipids constitute one of the main classes of glycosylated biosurfactants that have attracted interest because they are synthesized by non-pathogenic yeasts from glucose and vegetable oils at high titers. In this work, the self-assembly properties of several sophorolipids in water at high concentrations (20 – 80 wt%), a range so far mostly uncharted, have been investigated by polarized-light microscopy and X-ray scattering. Some of these compounds were found to show lyotropic liquid-crystalline behavior as they display lamellar or hexagonal columnar mesophases. X-ray scattering data shows that the structure of the lamellar phase is almost fully interdigitated, which is likely due to the packing difference between the bulky hydrophilic tails and the more compact aliphatic chains. A tentative representation of the molecular organization of the columnar phase is also given. Moreover, some of these compounds display thermotropic liquid-crystalline behavior, either pure or in aqueous mixtures. In addition, small domains of the lamellar phase can easily be aligned by applying them a moderate a.c. electric field, which is a rather unusual feature for lyotropic liquid crystals. Altogether, our work explored the self-assembly liquid-crystalline behavior of sophorolipids at high concentration, which could shed light on the conditions of their potential industrial applications as well as on their biological function.

1. INTRODUCTION

The expression “biological amphiphiles” commonly refers to molecules derived from natural resources and obtained by plant extraction, enzymatic synthesis, or microbial fermentation. This represents an important field of research and the corresponding compounds are also broadly known as “biosurfactants”, as their surface-active properties have been reported many years ago.¹⁻³ The best-known biosurfactants are glycosylated lipids (sophorolipids, rhamnolipids, mannosylerythritole lipids...) and derivatives of small peptides (surfactin), and they have been developed for decades to replace synthetic surfactants for their lower environmental impact.¹⁻³ Biosurfactants are indeed considered to be more biodegradable and less toxic than petrochemical surfactants, and therefore they find use in a number of applications in detergency, cosmetics, environmental science, or as antimicrobial compounds,⁴⁻⁶ with a milder effect on protein denaturation.⁷

Nonetheless, the word biosurfactant is slightly reductive, as these molecules often present a richer self-assembly and phase behavior than classical surfactants.^{8,9} The spontaneous self-assembly and above all the lyo- and thermotropic phase behavior of amphiphiles are features of paramount importance, as these determine their properties and potential field of application.¹⁰ On the one hand, the lyotropic phase behavior is presently known for most major kinds of amphiphiles, be they surfactants or lipids. On the other hand, the self-assembly properties of biological amphiphiles obtained by microbial fermentation have been studied only since the late 80's¹¹ and they generally only pertain to the study of diluted systems.⁸ Only mannosylerythritole lipids (MEL) have been studied at concentrations above 20 wt% by the group of Kitamoto et al., who mainly observed uni- and multilamellar vesicles below about 60 wt% and an L_{α} phase above

60 wt% for MEL-A, B, C, and D, except for MEL-A, which forms cubic (V2) and coacervate (L3) phases below 65 wt% and 55 wt%, respectively.¹²⁻¹⁷

There are several reasons why there is only a limited amount of work that addresses the lyotropic behavior of microbial amphiphiles. First of all, such studies require important amounts of material, which is hardly possible for most microbial fermentations. Secondly, they require high-enough purity and homogeneity, which is also a true challenge in the synthesis of this class of compounds. Furthermore, most microbial amphiphiles are sensitive to pH and ionic strength, which are two parameters hard to control at high concentrations.⁸ Interestingly, MELs do not have pH-sensitive chemical groups and could be obtained reasonably pure in high amounts. This is not the case of many other biosurfactants which, like rhamnolipids, contain a -COOH group and are generally produced as a mixture of mono and dirhamnolipids.¹⁸ Sophorolipids are also mixtures of the acidic and lactonic forms. Although the fully acidic form can be easily obtained by alkaline hydrolysis, inhomogeneity across batches has previously led to misinterpretation of their self-assembly properties.¹⁹ Fortunately, the recent advances in microbial fermentation from genetically-modified microorganisms has paved the way for the synthesis and high-amount production of a wide range of both old and new microbial amphiphiles.²⁰⁻²⁶

This work deals with the lyotropic phase behavior of several members of a series of sophorolipids (Figure 1), including not only the non-acetylated well-known open acidic form but also several other acetylated acidic and non-acidic bolaform sophorosides, bearing two symmetrical (or non-symmetrical) sophorose headgroups. Detailed investigations of these systems were made by combining polarized-light microscopy and X-ray scattering. Some members of this series were found to form lyotropic lamellar or columnar liquid-crystalline phases at high concentrations, and tentative models for their molecular organization are shown.

The lamellar phase is fluid enough to be readily aligned by moderate shear flow. Moreover, interestingly, lamellar domains growing from the isotropic liquid phase can also be aligned by applying a high-frequency, alternating-current, electric field, which is rather uncommon for lyotropic liquid crystals. Altogether, investigating the liquid-crystalline behavior of sphorolipids (and biosurfactants in general) not only helps improving our knowledge of their structure-properties relationship⁸ but also extends the field of liquid crystals to biosurfactants, which have original biocompatibility and functionality properties of great interest for biomedical applications.²⁷

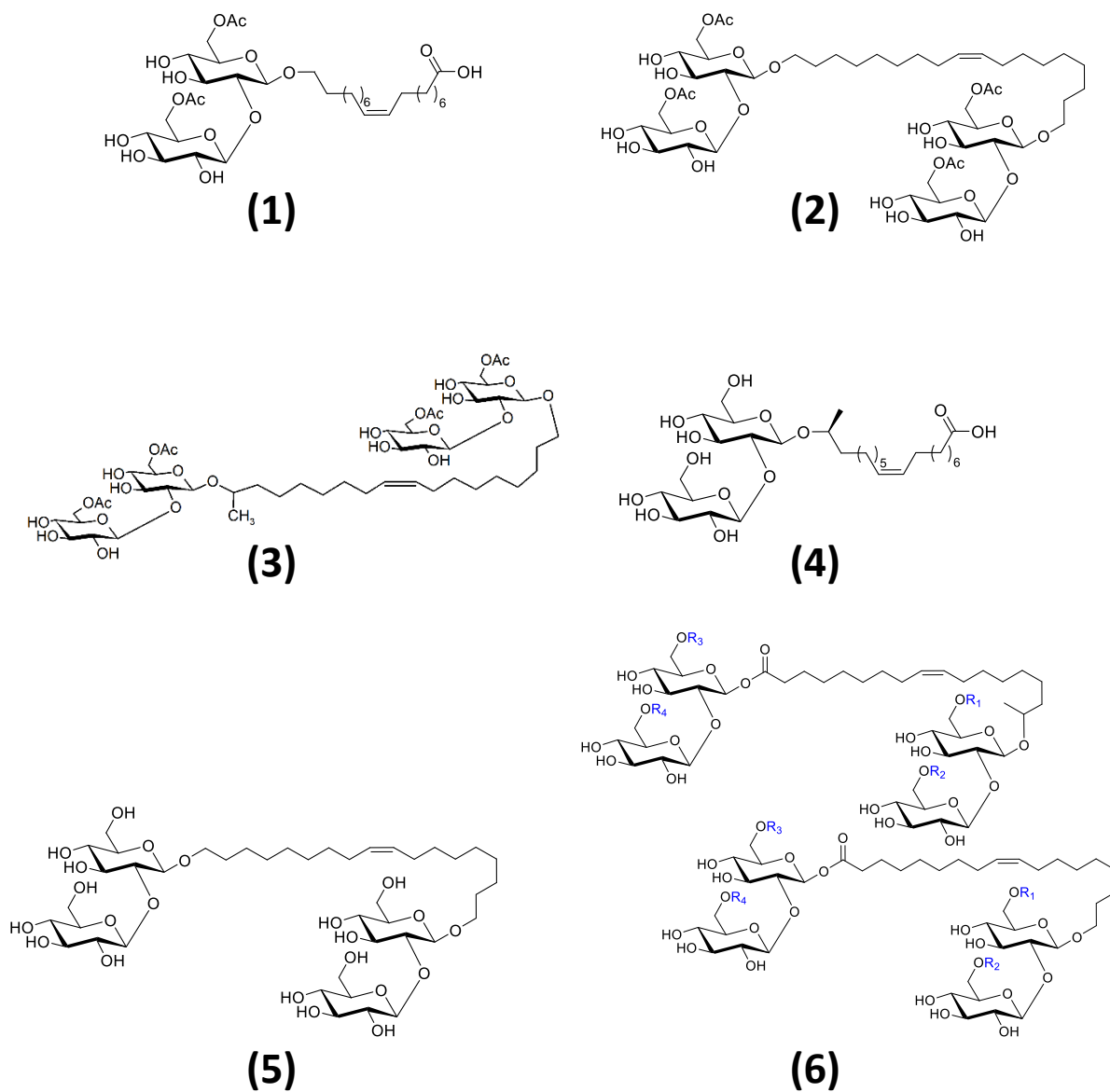


Figure 1. Sophorolipids studied in this work. (1) Di-acetylated acidic sophorolipids (C18:1, ω), (2) Tetra-acetylated symmetrical bola sophoroside (C18:1, ω); (3) Tetra-acetylated non-symmetrical bola sophoroside (C18:1, $\omega/\omega-1$); (4) Non-acetylated acidic sophorolipids (C18:1, $\omega-1$); (5) Non-acetylated symmetrical bola sophoroside (C18:1, ω); (6) (Non-)acetylated bola sophorolipid (C18:1, $\omega/\omega-1$) ($R_1 = R_2 = R_3 = R_4 = H$ or Ac).

2. MATERIALS AND METHODS

2.1. Synthesis. All sophorolipid samples used in this study have been purchased by the Bio Base Europe Pilot Plant (Gent, Belgium) and used as such without further purification. All samples have been produced by microbial fermentation within the framework of the APPLISURF project. For the sake of simplicity, all compounds are numbered here from (1) through (6) in Figure 1. However, their in-house and Applisurf project codes are listed in Table 1. All compounds are obtained from modified *S. bombicola* strains and their production and analysis have been described elsewhere (compounds 1 and 4 in Ref. ²⁴; compounds 2, 3, and 5 in Ref. ²³; compound 6 in Ref. ²⁶). All compounds except (1) were provided as dry powders. Compound (1), which contained 35 wt% dry matter upon delivery, has been freeze-dried in powder form prior to use. For all compounds, according to the specification sheet, non-glycolipid impurities (free fatty acids, glucose, glycerol, oil, proteins) are attested between 0.5 wt% and 1 wt% in the dry matter analysis, while the congener purity is attested above 95 %, according to relative peak area analysis of HPLC-ELSD chromatograms.

Table 1 – List of sophorolipid compounds used in this study

Compound name	N ^r	In-house code	Applisurf code	Reference
Di-acetylated acidic sophorolipids (C18:1, ω)	1	N106	Surfactant 66	²⁴
Tetra-acetylated symmetrical bola sophoroside (C18:1, ω)	2	N103	Surfactant 6	²³
Tetra-acetylated non-symmetrical bola sophoroside (C18:1, $\omega/\omega-1$)	3	N102	Surfactant 49	²³
Non-acetylated acidic sophorolipids (C18:1, $\omega-1$)	4	N300	Surfactant 5	²⁴
Non-acetylated symmetrical bola sophoroside	5	N101	Surfactant 1	²³

(C18:1, ω)				
(Non-)acetylated bola sophorolipid (C18:1, $\omega/\omega-1$) ($R_1 = R_2 = R_3 = R_4 = H$ or Ac)	6	N100	Surfactant 14	26

2.2. Sample preparation. All samples were prepared by precisely weighing the appropriate amount of sophorolipid dry powder in 2 mL glass vials equipped with tight Teflon-lined caps (or in 2 mL Eppendorf tubes) and adding the appropriate volume of de-ionized 18 M Ω .cm water. The concentration range of the sophorolipids varied between 20 wt% and 90 wt%. The samples, of typically 0.5 mL volume, were vortexed, sonicated in a standard ultra-sound bath, then heated at 60 °C for 3-5 min if necessary in an Eppendorf ThermoStat™ C, and left to equilibrate for several days at room temperature (or at \approx 60°C if necessary) until they were completely clear. All compositions are expressed in wt% (i.e. in g of biosurfactant per g of mixture).

The samples were then carefully examined both in natural light and between crossed polarizers to assess the sample homogeneity, the number of coexisting phases, and whether the phases are isotropic or birefringent (a strong hint of their liquid-crystalline character).

For more detailed investigations by optical microscopy, samples were filled into optical flat glass capillaries of 100 μ m thickness and 2 mm width (VitroCom NJ, USA). This was achieved either simply by capillarity for fluid enough samples or by gently sucking more viscous materials into capillaries using a small vacuum pump. Sometimes, very concentrated and visco-elastic samples had to be warmed at \approx 60-70 °C for this purpose. For some samples, “contact preparations” were also made by letting a small water drop touch the powder, between glass slide and coverslip, resulting in an unknown water concentration gradient, but also in clearer liquid-crystalline textures than for samples in capillaries. Moreover, the behavior of the samples upon heating was investigated using a heating stage (Mettler-Toledo).

2.3. Polarized-light microscopy. Observations by polarized-light microscopy were made with an Olympus BX51 polarizing microscope to try to identify the nature of the liquid-crystalline phases. The optical textures were recorded with a sCMEX-20 (Euromex, Netherlands) camera. In several cases, a wave-plate was also inserted to visualize the direction of the slow axis of some birefringent domains. A Berek crystalline compensator (Olympus U-CBE) was also used to measure the birefringence of some samples.

In some cases, the influence of an alternating-current (a.c.) sinusoidal electric field on the samples was also assessed by placing the optical capillaries in an already described homemade electro-optic cell directly placed on the microscope rotating stage.²⁸ The electrodes were 2-mm apart (SI Figure S1) and the voltage and frequency were typically 280 V_{rms} and 500 kHz, respectively. (A 1 Tesla magnetic field, delivered by rare-earth permanent magnets, was also applied to some of the samples but it had no effect.)

2.4. Structural study by X-ray scattering. Structural studies were also conducted to confirm the mesophase assignment by X-ray scattering. For this purpose, the samples were filled into 1-mm diameter Lindemann glass capillaries (diameter 0.9 mm, Glas-Technik & Konstruktion, Germany) by gentle centrifugation or with help of a small vacuum pump, and the capillaries were flame-sealed. Note that the flow that occurred during centrifugation could sometimes align fluid enough samples, in particular in the lamellar phase.

A versatile diffractometry apparatus which is part of the MORPHEUS X-ray scattering platform of Laboratoire de Physique des Solides was used. This apparatus is set on a copper rotating-anode X-ray generator (Rigaku, Japan, $\lambda_{\text{CuK}\alpha} = 1.541 \text{ \AA}$). The X-ray beam was focused and monochromatized by a W/Si multilayer mirror optics (Osmic). The scattered X-rays were

collected by a MAR-research 345 detector (marXperts GmbH, Germany) and the sample-to-detection distance was typically 300 mm, which provides an accessible q -range of $0.05\text{-}2\text{ \AA}^{-1}$, where $q = (4\pi\sin\theta)/\lambda$ is the scattering vector modulus and 2θ is the scattering angle. Exposure times were typically 30 min to 2 h long and the pixel size was $150\text{ }\mu\text{m}$. The 2-dimensional scattering patterns were azimuthally averaged with a home-made software to produce curves of scattered intensity versus scattering vector modulus, $I(q)$.

3. RESULTS AND DISCUSSION

3.1. Investigations of aqueous solutions of compound (1). Observations of a series of samples taken from solutions of compound (1) in water at concentrations starting from 20 wt%, between crossed polarizers, show that they are birefringent at 70 wt% and above. This indicates that 70 wt% is the threshold beyond which the solutions spontaneously organize in a liquid-crystalline phase. The textures observed by polarized-light microscopy are typical of a lamellar phase, although they depend on the sample composition. At 80 wt%, areas with focal conic domains, homeotropic areas with oily streaks, or spherulitic defects, are most often observed (Figure 2a,b) and are completely similar to those of other lyotropic lamellar phases.²⁹ In contrast, at 70 wt%, the samples are biphasic, with a small amount of solvent coexisting with the liquid-crystalline phase. The latter grows within the former as anisotropic rod-like birefringent domains (Figure 2c), called “bâtonnets de Friedel-Grandjean” (French for “Friedel and Grandjean rod-like objects”).³⁰ The microscopic organization of these objects, which are quite characteristic of the lamellar (or smectic A) mesophase, results both from the requirement

of keeping the lamellar period constant and from the director anchoring condition at the lamellar/isotropic liquid interface.^{31,32}

By using an optical compensator, the birefringence of a small aligned part of the sample, Δn , was estimated to be on the order of 6×10^{-4} , which, taking the dilution into account, provides the value of the specific birefringence of the biosurfactant membranes, $\Delta n_{sp} \approx 8 \times 10^{-4}$. This value is lower than that, $\Delta n_{sp} \approx 4 \times 10^{-3}$, reported for the sodium decylsulfate anionic surfactant system,³³ which might suggest a larger conformational disorder of the biosurfactant compound (1), or could be due to the sample being only partially aligned.

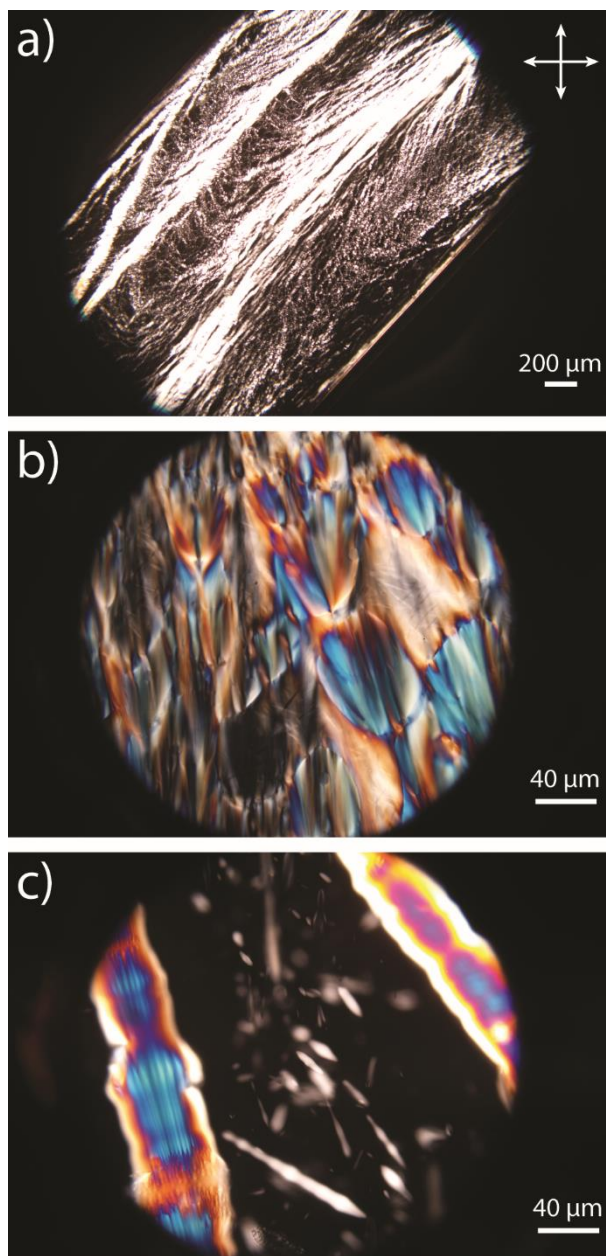


Figure 2 - Polarized-light microscopy images of aqueous mixtures of compound (1) in flat glass capillaries. a) Oily streaks (80 wt%); b) Focal conics (80 wt%); c) Bâtonnets de Friedel-Grandjean embedded in the isotropic liquid (70 wt%). The crossed polarizer and analyzer are shown in a).

The X-ray scattering patterns of solutions of compound (1) at 70 wt% (in the birefringent part) are indeed typical of a lamellar liquid-crystalline phase (Figure 3). At wide scattering angles, a

broad scattering ring is observed and shows that the aliphatic tails of the surfactant molecules are in a molten state, which ensures the fluidity of the mesophase. At small angles, two sharp (001) and (002) reflections are observed, with $q_{002} = 2q_{001}$, and classically correspond to the diffraction by the smectic layers. As usual, the second-order smectic reflection is much weaker than the first one, but it is nevertheless easily detected (Figure 3). The number of lamellar reflections visible on the scattering pattern may appear unusually small, compared to common ionic surfactants. However, the acidic form of sophorolipids should rather be compared with non-ionic surfactants,^{34,35} the patterns of which usually display much fewer reflections. This means that the microsegregation of the polar and apolar parts of compound (1) is weak, resulting in a lamellar phase subject to a high level of positional fluctuations (that are not shown in the schematic sketch of Figure 4).

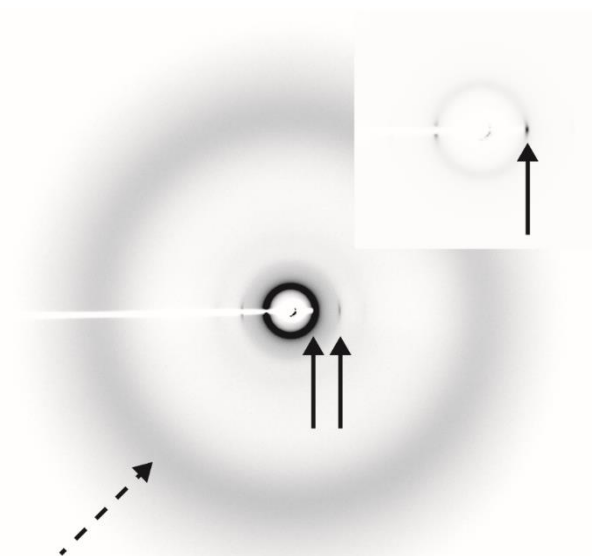


Figure 3. X-ray scattering pattern of compound (1) at 70 wt%. The inset at the top-right shows the underexposed central part of the pattern. The solid black arrows point to the first and second-order lamellar reflections whereas the dashed black arrow points to the wide angle diffuse ring.

Moreover, the phase was aligned by the centrifugation of the sample at the bottom of the X-ray capillary tube, resulting in sharp smectic reflections rather than an isotropic sharp diffraction ring. The orientation of the smectic reflections shows that the smectic layers are aligned with their normal parallel to the capillary axis. The smectic period, $d = 36 \pm 1 \text{ \AA}$, is simply obtained from the relation $d = 2\pi/q_{001}$. Furthermore, the thickness, δ , of the surfactant membrane can be derived from the classical relation, $d = \delta/\phi$, between d , δ , and the surfactant volume fraction, ϕ , which directly results from the geometry of the lamellar phase. With $\phi = 70\%$ (that is, assuming a density close to 1), this leads to $\delta = 26 \pm 1 \text{ \AA}$. Estimations of the molecular length, l , of compound (1) in an extended conformation give $l = 30 \pm 4 \text{ \AA}$,^{8,34,36} so that $\delta \approx l$. (The large uncertainty on l comes from the presence of the double bond, the bending of the oleic acid chain and the pH at which experiments were made, refer to Table 7 in Ref. ⁸). This means that the surfactant membranes of (1) in the lamellar mesophase are not bilayered, as intuitively expected, but single-layered and the structure is therefore interdigitated (Figure 4). In a single membrane, there are as many molecules pointing in one direction (along the normal to the membrane) as in the opposite one, and both the sugar heads and the terminal acid groups are located close to the aqueous medium, effectively shielding it from the aliphatic parts of the molecules. This is consistent with the interdigitated membrane structure found for similar single-glucose biosurfactants forming both flat and vesicular membranes.^{36,37}

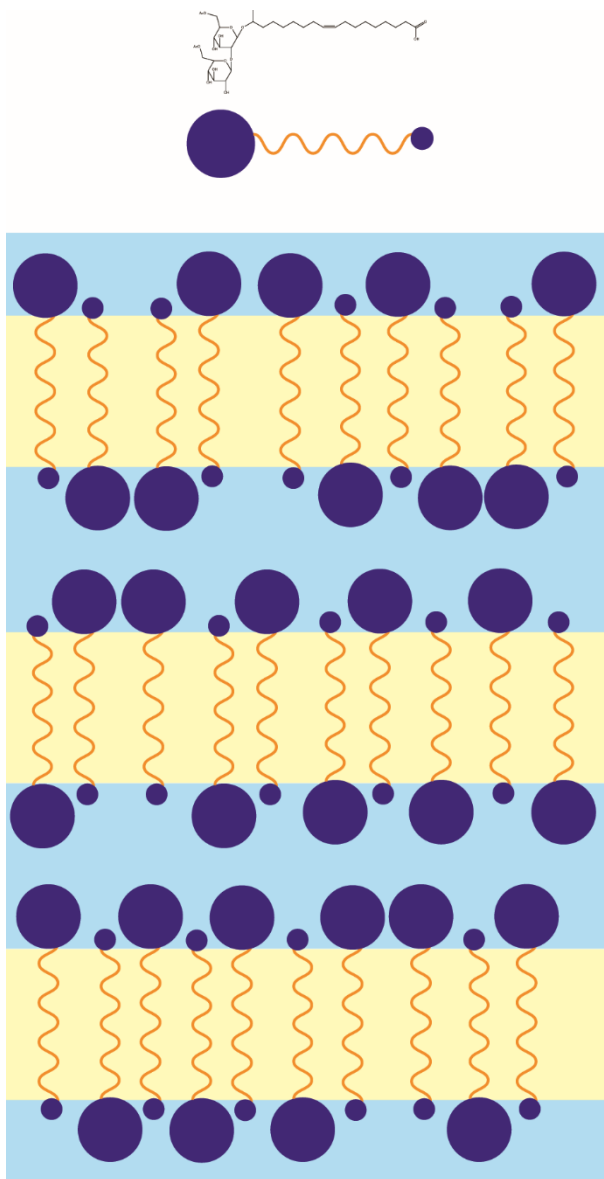


Figure 4. Tentative schematic of the molecular organization of compound (1) in the interdigitated lamellar mesophase. The hydrophilic and hydrophobic media are respectively shown in light blue and light yellow. (For clarity, only a few molecules have been represented. Their conformation does not result from any calculation and their intrinsic conformational disorder is not shown.)

An investigation of the thermal behavior of compound (1) by polarized-light microscopy revealed that it also has thermotropic properties. Indeed, upon heating, the pure powder melts at

$\approx 140^\circ\text{C}$ to form the lamellar phase, which then turns isotropic at $\approx 150^\circ\text{C}$. The lamellar period $d = 29.4 \text{ \AA}$, measured from the X-ray scattering pattern, confirms our previous estimate of the molecular length. Liquid-crystalline compounds that present both lyotropic and thermotropic behaviors are called amphitropic. These compounds often form hydrogen bonds and some of them are in fact bolaform amphiphiles, such as cerebrosides.³⁸ Therefore, in this context, the observation of the amphitropic behavior of the sophorolipid (1) is not quite unexpected. The transition temperatures are lower, respectively 40°C and 70°C , for the aqueous mixtures with concentration ranging from 70 wt% to 85 wt%, with very little dependence on this parameter in this range.

Finally, the influence of an a.c. electric field on the lamellar phase of the aqueous mixtures of (1) was examined. Indeed, although this kind of experiment is quite uncommon with lyotropic mesophases of surfactants, we are used to applying electric fields to lyotropic liquid-crystalline dispersions of rod-like or disk-like particles to grow single domains, thanks to original set-ups developed for this purpose.²⁸ The effect of the electric field is most clearly seen at the highest possible dilution (i.e. 70 wt%) at which the bâtonnets de Friedel-Grandjean coexist with excess solvent. For example, a small bâtonnet lying initially at about 45° with respect to the direction of application of the field (Figure 5a) was selected. When the field is applied, the bâtonnet rotates in only a few seconds to realign its revolution symmetry axis perpendicular to the field (Figure 5b,c). Because the smectic layers are mostly perpendicular to the axis of the bâtonnet,³¹ this observation means that the anisotropy of electric permittivity, $\Delta\epsilon$, of the lamellar phase is negative. Moreover, $\Delta\epsilon$ is large enough for a rather moderate electric field of $\approx 0.15 \text{ V}/\mu\text{m}$ to realign the bâtonnet within short times. (Note that this reorientation effect of the whole lamellar bâtonnet in the isotropic matrix should not be interpreted as a field-induced distortion of the

lamellar structure similar to the well-known Fréedericksz transition of nematics.) Besides, the size of the bâtonnet also markedly decreased, which could be due to the melting of the lamellar phase because the high conductivity of the suspension ($\text{pH} \approx 4$) could give rise to Joule heating.

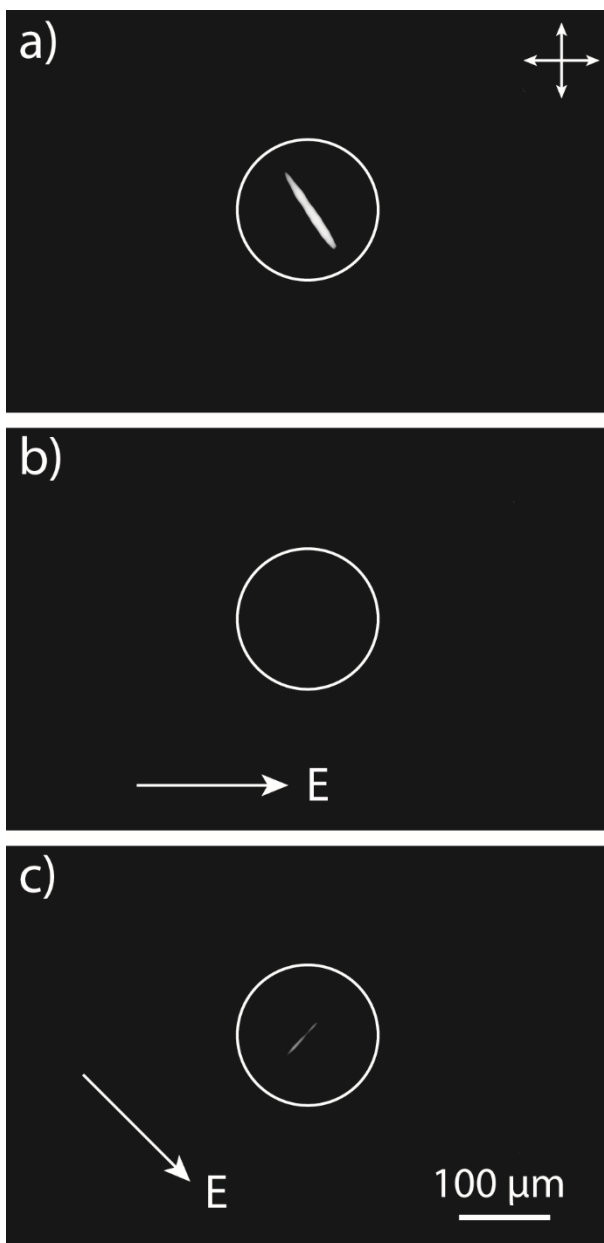


Figure 5. Rotation of a “bâtonnet de Friedel-Grandjean” of compound (1) submitted to an electric field. a) No field applied, horizontal capillary. The bâtonnet lies at ca 45° with respect to the polarizer direction. b) Under field (500 kHz, $0.15 \text{ V}/\mu\text{m}$), the bâtonnet rotates so that its main

axis lies perpendicular to the field (i.e. vertical), making it invisible between crossed polarizers.

c) Rotating the stage by 45° reveals the bâtonnet, with axis perpendicular to the field.

3.2. Investigations of aqueous solutions of compound (2). The aqueous mixtures of compound (2), which bears two hydrophilic heads, are also birefringent for concentrations of 70 wt% and above. Their optical textures, observed by polarized-light microscopy, definitely suggest the presence of a liquid-crystalline phase (Figure 6a). However, because of the large viscoelasticity of the mesophase, its texture in flat glass capillaries does not coarsen much with time, which prevents proper identification of its nature. Although the assignment as a nematic phase seems quite unlikely, an ambiguity remains between the lamellar and the columnar phases that can sometimes display rather similar textures in the case of large defect densities.

To solve this problem, a water drop was directly deposited in contact with a few grains of biosurfactant powder, between glass slide and coverslip. One crucial advantage of this method, compared to commercial flat glass capillaries, is that a much thinner sample is obtained, which leads to clearer textures, although two salient drawbacks are that the preparation shows an unknown concentration gradient and the sample is out of equilibrium, as the two components diffuse within each other and the whole preparation slowly dries. Nevertheless, detailed microscopic observations of the texture thus prepared allowed us to identify small but clear-cut developable domains (Figure 6b) that are the signature of the presence of a columnar mesophase.³⁹

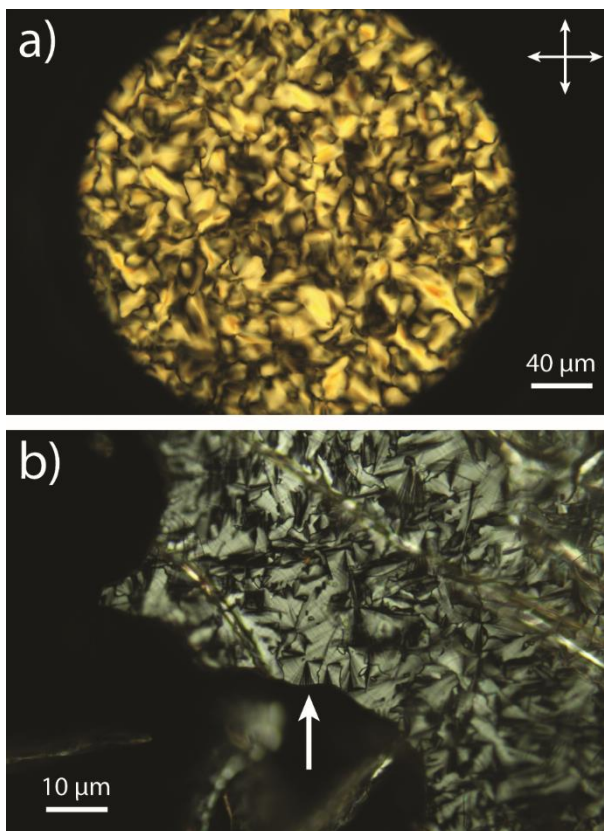


Figure 6. Polarized-light microscopy images of aqueous mixtures of compound (2). a) Liquid-crystalline texture at 80 wt%; b) Contact preparation of the crystalline powder with water showing developable domains (white arrow). The crossed polarizer and analyzer are shown in a).

The texture of samples in flat glass capillaries somewhat coarsened after 6 months, so that small aligned areas were found, allowing us to estimate the phase birefringence. The value obtained, $\Delta n \approx 2.5 \times 10^{-3}$, is again comparable to the few values already reported in literature for lyotropic liquid-crystals of synthetic surfactant molecules.³³ It is larger than that reported above for the lamellar phase but this difference might only reflect different alignment qualities.

The X-ray scattering study of the aqueous mixtures of compound (2) confirms the assignment as a hexagonal columnar mesophase (Figure 7). In contrast with that in Figure 3, the scattering

pattern here is perfectly isotropic, which shows that the phase is too viscoelastic to be aligned by the usual capillary filling process (note however that the mesophase could be partially aligned by achieving a strong flow in a capillary).

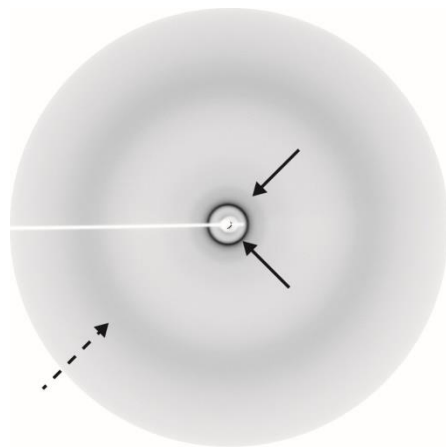


Figure 7. X-ray scattering pattern of compound (2) at 70 wt%. The solid black arrows point to the (10) and (11) reflections of the hexagonal lattice and the dashed black arrow points to the wide angle diffuse ring.

At wide angles, a broad scattering ring is observed, which shows the fluid character of the mesophase. At low angles, two rather sharp diffraction rings are observed at $q_{10} = 0.216 \text{ \AA}^{-1}$ and $q_{11} = 0.382 \text{ \AA}^{-1}$. The ratio of these two values ($q_{11}/q_{10} = 1.77$) is close enough to $\sqrt{3}$ to identify the mesophase as a hexagonal columnar phase. The low-angle diffraction rings of the columnar phase are broader than those of the lamellar phase, which suggests a smaller coherent domain size for the former phase, in line with the microscopic texture observations. The position of the hexagonal (10) reflection provides the hexagonal lattice parameter: $a = \frac{2\pi}{q_{10}} \frac{2}{\sqrt{3}} = 34 \pm 1 \text{ \AA}$, at 70 wt%.

The scattering pattern (SI Figure S2) of the sample at 80 wt% is very similar to that in Figure 7, except that the low-angle diffraction lines are slightly better defined and that the lattice parameter is somewhat smaller due to the lower water content. Moreover, a few, quite faint, sharp diffraction rings can be detected at wide scattering angles, suggesting the presence of a small proportion of crystalline phase in equilibrium with the mesophase.

In principle, the structural data alone does not allow determining whether the columnar phase is direct (with water outside the columns and the aliphatic tails buried within the columns) or inverse (with water and polar head-groups buried deep in the columns). However, the comparison of the molecular structures of compounds (1) and (2) suggests that the columnar phase is direct. Indeed, the lamellae of the interdigitated smectic phase of compound (1) do not have any spontaneous curvature (Figure 4), as expected for a lamellar phase,^{40,41} which means that the hydrocarbon chain cross-section area (typically $\approx 0.2 \text{ nm}^2$) is about half that of the polar head. Because compound (2) has two polar heads per chain, we argue that the polar heads must occupy more space than the chains at the chain/head interface, leading to its curvature and the formation of a direct mesophase structure (Figure 8).

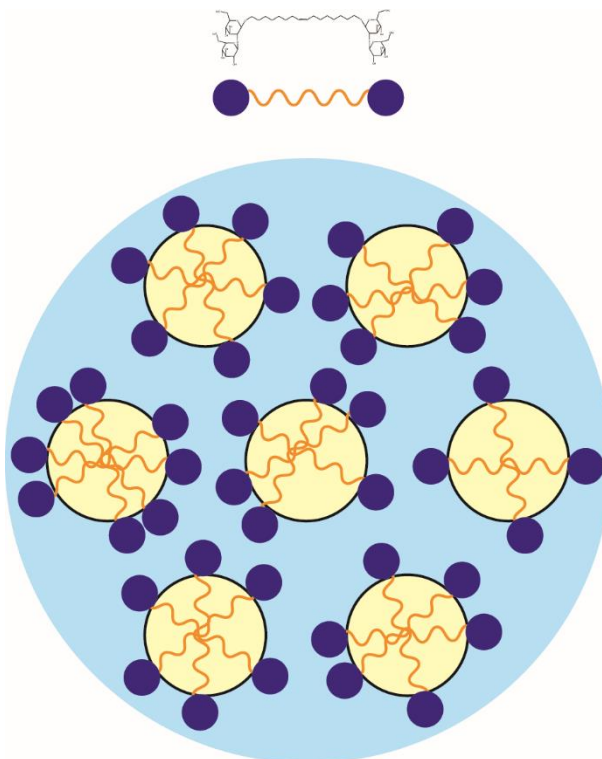


Figure 8. Tentative schematic of the molecular organization of compound (2) in the hexagonal columnar mesophase. The hydrophilic and hydrophobic media are respectively shown in light blue and light yellow. (For clarity, only a few molecules have been represented. Their conformation does not result from any calculation and their intrinsic conformational disorder is not shown.)

The thermal behavior of both the pure compound (2) and its aqueous mixtures were also investigated by polarized-light microscopy. In sharp contrast with compound (1), the crystalline powder of compound (2) melts directly in the isotropic phase, meaning that the pure compound (2) has no thermotropic properties. However, temperature has some influence on its aqueous mixtures since the columnar phase melts upon heating into the isotropic phase, with a clearing

point that increases slightly from $\approx 45^\circ\text{C}$ at 70 wt% to $\approx 55^\circ\text{C}$ at 85 wt%. Finally, no alignment effect of an a.c. electric field on the columnar mesophase was observed.

3.3 Investigations of aqueous solutions of compound (3). This compound only differs from compound (2) by a lateral methyl substitution on the aliphatic chain, close to one of the two hydrophilic heads. This substitution seems to have little influence on the mesomorphic properties because the aqueous mixtures of compound (3) behave much like those of (2) in this respect. Indeed, only the mixtures of weight fraction 70 wt% and above are birefringent and their textures, observed by polarized-light microscopy, are also typical of either a lamellar or a columnar mesophase (SI Figure S3). However, the X-ray scattering patterns (SI, Figure S4) display two reflections the scattering vectors of which are in a ratio $q_{11}/q_{10} \approx \sqrt{3}$, which strongly suggests that the mesophase is columnar with hexagonal symmetry, just like compound (2). The hexagonal lattice parameter is $a = 33 \pm 1 \text{ \AA}$, at 70 wt%, which is the same, within error bars, as for (2). Then, the methyl substitution has no effect on the lyotropic mesomorphism.

3.4 Investigations of aqueous solutions of compound (4). The aqueous mixtures of compound (4) are biphasic at concentrations from 60 wt% and above, since the observation of their textures reveals the presence of small birefringent spherical droplets floating in an isotropic liquid matrix (SI Figure S5). In contrast with lamellar spherulitic topological defects, the droplets are readily visible in natural light. This texture is highly reminiscent of that of the so-called “onion phase” of strongly sheared lamellar phases, where the lamellar structure is broken up in multi-lamellar vesicles (MLVs).⁴²

The scattering patterns of the aqueous mixtures of compound (4) (SI Figure S6) display, at wide angles, the usual broad scattering peak showing that the coexisting phases are fluid and, at low angles, a strong peak (at $q_0 = 0.23 \text{ \AA}^{-1}$) that is not as sharp as that observed with (1) in the lamellar phase. This might be due to the small size of the droplets. Moreover, higher-order reflections at positions close to $2q_0$, $3q_0$, and $4q_0$ are barely guessed on the scattering pattern, which would confirm that the spherulites are in a lamellar phase. The lamellar period, $d = 2\pi/q_0 = 27.5 \pm 1 \text{ \AA}$ remains almost constant, whatever the concentration, as if the lamellar phase could only incorporate a very small amount of solvent. Indeed, this period is close to the thickness, $\delta = 26 \text{ \AA}$, of the membranes of (1) (see above). At this stage, we see no reason why compound (4) should be less hydrophilic than compound (1) and, moreover, our assignment of this phase as probably lamellar still requires confirmation.

3.5 Investigations of aqueous solutions of compounds (5) and (6). The aqueous mixtures of compound (5) show homogeneous birefringent textures at concentrations of 60 wt% and above but these mixtures are so visco-elastic that the textures hardly coarsen and the defects cannot be studied in detail, preventing phase identification. At 60 wt%, the X-ray scattering pattern shows the wide-angle diffuse ring and a low-angle strong, yet rather broad, peak at $q_0 = 0.22 \text{ \AA}^{-1}$ ($d = 28 \pm 1 \text{ \AA}$). Although the absence of clear higher-order peaks again prevents proper identification of this liquid-crystalline phase, one can still reasonably exclude any isotropic cubic (V2) or sponge (L3) phase, due to the marked birefringence of the sample. Phase assignments as lamellar, or columnar (or even nematic), displaying various kinds and degrees of disorder would all be consistent with this data. At 70 and 80 wt%, the scattering patterns also display sharp peaks at wide angles, which is the sign of the onset of crystallization.

Finally, all aqueous mixtures of compound (6) at concentrations up to 80 wt% are optically isotropic and no liquid-crystalline properties have been observed.

3.6 General discussion. Table 2 summarizes the liquid-crystalline behavior of sophorolipids (1) to (6). As a general trend, most compounds form liquid-crystalline phases at concentrations above ca 60-70 wt%. This is somewhat higher than the concentrations (ca 30-60 wt%) most often reported for the onset of liquid-crystallinity in binary systems of water and other non-ionic, anionic, cationic surfactants, and lipids.⁴³⁻⁴⁶ Each sophorolipid forms a single mesophase (if any), lamellar or columnar, in contrast with most usual surfactants since the latter frequently show multiple phases, depending on concentration. This could be due to the narrower concentration range of mesophase stability of the sophorolipids. Furthermore, it seems that acidic sophorolipids, acetylated or not, tend to self-assemble into lamellae that can be flat in the lamellar phase of the diacetylated compound (1) or curved in multilamellar vesicle (MLV) phase of its non-acetylated homologue (4). In both cases, the lamellae have an interdigitated structure. Interestingly, flat membranes, vesicles or even MLV, have been observed before, although at much lower concentrations (< 5 wt%), not only for single-glucose C18:1 and C18:0 microbial bioamphiphiles,^{36,37} but also for branched derivatives of sophorolipids containing a C22 fatty acid.⁴⁷ Although little is known, due to lack of studies, in terms of liquid-crystalline behavior of other biosurfactants at comparable (high) concentrations, hydroxyl groups appear to have a similar effect on the stabilization of MLV. Mannosylerythritole lipids, produced by the yeast strain *C. antarctica*, are commonly isolated in four different congeners, differing by the acetylation degree and position of the acetyl group. The fully acetylated congener, MEL-A, was shown to form coacervate (L3) and cubic (V2) phases below ≈ 65 wt% in water, whereas the

partially de-acetylated (MEL-B, MEL-C) and the non-acetylated (MEL-D) congeners rather form MLV in the same concentration range.^{12,13,15,48} All compounds seemed to stabilize an L_{α} phase above 65 wt% (for a summary of the phase diagram of MELs, refer to Tables 5 and 6 in Ref. 8). The role of the acetyl group on the C6 of sophorose in decreasing membrane curvature could probably be explained in terms of its hydrophobic character. Indeed, for cationic alkylammonium surfactants, it has already been reported that, although the triethylammonium headgroup drives morphologies with high curvatures (e.g., micellar cubic), in line with the packing parameter theory,⁴⁹ larger headgroups like tripropyl or tributylammonium, show the opposite trend as they stabilize flatter structures.⁵⁰ This was explained by the increasingly hydrophobic character of the headgroup. Finally, the interdigitated structure of the membranes was expected, based on the bolaform, although asymmetric, character of sophorolipids. Interdigitated structures have been observed for other microbial biosurfactants, like C18:1 and C18:0 glucolipids,^{36,37} surfactin⁵¹ or rhamnolipids⁵², and they are actually predicted by theoretical models of self-assembly of bolaform amphiphiles.⁵³

Compounds (2), (3), (5) and (6) are all sophorolipids bearing two symmetrical sophorose headgroups, instead of a sophorose and a carboxylic acid group for compounds (1) and (4). More specifically, compounds (2), (3), and (5) are sophorosides, owing to the glycosidic bond between the fatty acid and both sophorose groups, whereas (6) is a sophorolipid, owing to the glycosidic and ester bonds with sophorose on each side of the fatty acid. In Table 1, (2) and (3) are respectively labelled symmetrical and non-symmetrical, due to the ω and $\omega-1$ link with one of the sophorose headgroups. However, as mentioned above, they show the same mesomorphism, which indicates that such a slight structural variation has little influence on the self-assembly properties. Compared to (5), compounds (2) and (3) are both di-acetylated. Acetylation therefore

seems to favor the columnar phase (Table 2), with a probable direct character (i.e. with the glycolipids inside the columns, Figure 8). Furthermore, the full hydroxylation of (5) leads to a mesophase whose poor long-range order and high density of defects prevent its identification. Comparison with literature is limited by the lack of data on similar compounds, especially at high concentration. Although several microbial and synthetic bolaform sophorolipids and sophorosides similar to (2), (3), and (5) have already been studied,^{23,54–57} the concentrations explored were generally below 5-10 wt%, with rare exceptions.²³ Most of these molecules were found to self-assemble into micelles or semi-crystalline fibers, like a broader variety of synthetic glycosylated and non-glycosylated bolamphiphiles.⁵⁸ Despite such major differences, an interesting result has been reported by Gross *et al.* about the effect of acetylation on the self-assembly properties of non-, partial-, and fully-acetylated sophorolipid-functionalized zinc porphyrin bolaform complexes. Despite the strongly diluted conditions (μM to mM range), it was still shown that the fully-acetylated compound forms micelles whereas the partial and non-acetylated compounds form J-type, columnar, aggregates.⁵⁶

Table 2 – Summary of the liquid-crystalline behavior of sophorolipids (1) to (6)

Compound	< 60-70 wt%	> 60-70 wt%	Comments	Thermotropic/ electric
(1), (4)	Not birefringent	Lamellar	(4) rather forms onion-like spherulites (MLV)	(1) Yes/Yes (4) not tested
(2), (3)	Not birefringent	Columnar	Hexagonal (probably direct)	No/No
(5)	Not birefringent	Unidentified phase	Isotropic phases excluded, but crowded textures and poor X-ray patterns prevent identification	No/No
(6)	Not birefringent	Not birefringent	-	No

Finally, compound (6) only shows an isotropic phase in a broad concentration range, with crystallization occurring above 80 wt%. Since this specific material is in fact a mixture of congeners, little can be inferred about the structure-property relationship.

4. CONCLUSION

This study shows that sophorolipids can self-assemble in lyotropic liquid-crystalline phases of lamellar and columnar symmetry, just like synthetic surfactants and lipids do. Polarized-light microscopy and X-ray scattering investigations have indeed revealed optical textures and scattering patterns that are typical of these phases. The lamellar phase is less visco-elastic than the columnar phase and therefore grows as large domains that often show homeotropic anchoring in untreated flat glass capillaries. Moreover, it is readily aligned not only by shear flow but also by an a.c. electric field when it grows as bâtonnets from the isotropic liquid, which is rather uncommon for synthetic amphiphiles. The liquid-crystalline phases can never be diluted below 60 wt% but some of the sophorolipids studied and their aqueous mixtures display thermotropic behavior.

Overall, the experimental investigation of these systems is somewhat more demanding than that of synthetic surfactants due to the large biosurfactant concentrations required for formation of the liquid-crystalline phases. Consequently, the samples are often so visco-elastic that they are difficult to homogenize and to fill into capillaries. The large visco-elasticity of the samples also affects the quality of the data obtained by optical microscopy and X-ray scattering, due to large defect densities preventing proper texture identification and possibly broadening the diffraction lines. To solve this problem, resorting to high-temperature annealing is a common strategy. However, prolonged annealing at high temperature should be used here with great care because it

can induce conformational changes of the biosurfactant molecules.⁵⁹ These changes can take months of aging at room temperature to be reversed, if ever. Besides, pH is another important parameter because of the presence of acidic functional groups and its influence on the mesomorphism would deserve additional investigations.

Nevertheless, despite these experimental difficulties, exploring the phase behavior of sophorolipids in water at high concentrations is worth the effort as it may shed light on their structure-properties relationship, which remain poorly understood nowadays. It may also help developing a new generation of glycosylated, biocompatible, liquid-crystalline colloids (e.g., cubosomes, hexosomes) with potential applications in the fields of drug delivery and biosensing.²⁷ In addition, this work might provide a new perspective on the biological function of sophorolipids. Indeed, a recent study has shown that these compounds could represent an extra-cellular energy storage form in yeasts⁶⁰ and the highly dense and efficient molecular packing of liquid-crystalline phases may be an important advantage in this respect.

ASSOCIATED CONTENT

Supporting Information

Schematic of the electro-optic cell; X-ray scattering patterns of compounds (2) at 80 wt%, (3) at 70 wt%, and (4) at 70 wt%; polarized-light microscopy images of compounds (3) at 80 wt% and (4) at 70 wt%.

ACKNOWLEDGMENTS

Claire Goldmann (LPS, Université Paris-Saclay, CNRS) and Stéphan Rouzière (LPS-Plateforme Morpheus, Université Paris-Saclay, CNRS) are kindly acknowledged for, respectively, in-lab support and assistance with the X-ray scattering experiments.

Financial support. VLAIO (Agentschap Innoveren & Ondernemen, Flanders Region, Belgium), Intercluster Vis Project AppliSurf: HBC.2017.0704. We gratefully acknowledge funding from the French Agence Nationale de la Recherche (ANR), project SELFAMPHI –19-CE43-0012-01.

REFERENCES

- (1) Desai, J. D.; Banat, I. M. Microbial Production of Surfactants and Their Commercial Potential. *Microbiol. Mol. Biol. Rev.* **1997**, *61*, 47–64.
- (2) Mohanty, S. S.; Koul, Y.; Varjani, S.; Pandey, A.; Ngo, H. H.; Chang, J.-S.; Wong, J. W. C.; Bui, X.-T. A Critical Review on Various Feedstocks as Sustainable Substrates for Biosurfactants Production: A Way towards Cleaner Production. *Microb. Cell Fact.* **2021**, *20*, 1–13.
- (3) Vieira, I. M. M.; Santos, B. L. P.; Ruzene, D. S.; Silva, D. P. An Overview of Current Research and Developments in Biosurfactants. *J. Ind. Eng. Chem.* **2021**, *100*, 1–18.
- (4) Mishra, S.; Lin, Z.; Pang, S.; Zhang, Y.; Bhatt, P.; Chen, S. Biosurfactant Is a Powerful Tool for the Bioremediation of Heavy Metals from Contaminated Soils. *J. Hazard. Mater.* **2021**, *418*, 126253.
- (5) Shu, Q.; Lou, H.; Wei, T.; Liu, X.; Chen, Q. Contributions of Glycolipid Biosurfactants and Glycolipid-Modified Materials to Antimicrobial Strategy: A Review. *Pharmaceutics* **2021**, *13*, 227.
- (6) Moldes, A. B.; Rodríguez-López, L.; Rincón-Fontán, M.; López-Prieto, A.; Vecino, X.; Cruz, J. M. Synthetic and Bio-Derived Surfactants versus Microbial Biosurfactants in the Cosmetic Industry: An Overview. *Int. J. Mol. Sci.* **2021**, *22*, 2371.
- (7) Otzen, D. E. Biosurfactants and Surfactants Interacting with Membranes and Proteins: Same but Different? *Biochim. Biophys. Acta - Biomembr.* **2017**, *1859*, 639–649.
- (8) Baccile, N.; Seyrig, C.; Poirier, A.; Castro, S. A.; Roelants, S. L. K. W.; Abel, S. Self-Assembly, Interfacial Properties, Interactions with Macromolecules and Molecular Modelling and Simulation of Microbial Bio-Based Amphiphiles (Biosurfactants). A Tutorial Review. *Green Chem.* **2021**, *23*, 3842–3944.
- (9) Dhasaiyan, P.; Prasad, B. L. V. Self-Assembly of Bolaamphiphilic Molecules. *Chem. Rec.* **2017**, *17*, 597–610.
- (10) Tadros, T. *Encyclopedia of Colloid and Interface Science*; Springer-Verlag: Berlin Heidelberg, 2013.
- (11) Ishigami, Y.; Gama, Y.; Nagahora, H.; Yamaguchi, M.; Nakahara, H.; Kamata, T. The PH-Sensitive Conversion of Molecular Aggregates of Rhamnolipid Biosurfactant. *Chem. Lett.* **1987**, *16*, 763–766.
- (12) Imura, T.; Yanagishita, H.; Kitamoto, D. Coacervate Formation from Natural Glycolipid: One Acetyl Group on the Headgroup Triggers Coacervate-to-Vesicle Transition. *J. Am. Chem. Soc.* **2004**, *126*, 10804–10805.
- (13) Imura, T.; Hikosaka, Y.; Worakitkanchanakul, W.; Sakai, H.; Abe, M.; Konishi, M.; Minamikawa, H.; Kitamoto, D. Aqueous-Phase Behavior of Natural Glycolipid Biosurfactant Mannosylerythritol Lipid A: Sponge, Cubic, and Lamellar Phases. *Langmuir* **2007**, *23*, 1659–1663.
- (14) Arutchelvi, J. I.; Bhaduri, S.; Uppara, P. V.; Doble, M. Mannosylerythritol Lipids: A Review. *J. Ind. Microbiol. Biotechnol.* **2008**, *35*, 1559–1570.
- (15) Worakitkanchanakul, W.; Imura, T.; Fukuoka, T.; Morita, T.; Sakai, H.; Abe, M.; Rujiravanit, R.; Chavadej, S.; Minamikawa, H.; Kitamoto, D. Aqueous-Phase Behavior and Vesicle Formation of Natural Glycolipid Biosurfactant, Mannosylerythritol Lipid-B. *Colloids Surfaces B Biointerfaces* **2008**, *65*, 106–112.
- (16) Fukuoka, T.; Yanagihara, T.; Imura, T.; Morita, T.; Sakai, H.; Abe, M.; Kitamoto, D.

- Enzymatic Synthesis of a Novel Glycolipid Biosurfactant, Mannosylerythritol Lipid-D and Its Aqueous Phase Behavior. *Carbohydr. Res.* **2011**, *346*, 266–271.
- (17) Fukuoka, T.; Yanagihara, T.; Ito, S.; Imura, T.; Morita, T.; Sakai, H.; Abe, M.; Kitamoto, D. Reverse Vesicle Formation from the Yeast Glycolipid Biosurfactant Mannosylerythritol Lipid-D. *J. Oleo Sci.* **2012**, *61*, 285–289.
- (18) Moutinho, L. F.; Moura, F. R.; Silvestre, R. C.; Romão-Dumaresq, A. S. Microbial Biosurfactants: A Broad Analysis of Properties, Applications, Biosynthesis, and Techno-Economical Assessment of Rhamnolipid Production. *Biotechnol. Prog.* **2021**, *37*, 1–14.
- (19) Dhasaiyan, P.; Le Griel, P.; Roelants, S.; Redant, E.; Van Bogaert, I. N. A.; Prevost, S.; Prasad, B. L. V.; Baccile, N. Micelles versus Ribbons: How Congeners Drive the Self-Assembly of Acidic Sophorolipid Biosurfactants. *ChemPhysChem* **2017**, *18*, 643–652.
- (20) Geys, R.; De Graeve, M.; Lodens, S.; Van Malderen, J.; Lemmens, C.; De Smet, M.; Mincke, S.; Van Bogaert, I.; Stevens, C.; De Maeseneire, S.; et al. Increasing Uniformity of Biosurfactant Production in *Starmerella Bombicola* via the Expression of Chimeric Cytochrome P450s. *Colloids and Interfaces* **2018**, *2*, 42.
- (21) Saerens, K. M. J.; Roelants, S. L.; Van Bogaert, I. N.; Soetaert, W. Identification of the UDP-Glucosyltransferase Gene UGT1A1, Responsible for the First Glucosylation Step in the Sophorolipid Biosynthetic Pathway of *Candida Bombicola* ATCC 22214. *FEMS Yeast Res.* **2011**, *11*, 123–132.
- (22) Wang, H.; Roelants, S. L. K. W.; To, M. H.; Patria, R. D.; Kaur, G.; Lau, N. S.; Lau, C. Y.; Van Bogaert, I. N. A.; Soetaert, W.; Lin, C. S. K. *Starmerella Bombicola*: Recent Advances on Sophorolipid Production and Prospects of Waste Stream Utilization. *J. Chem. Technol. Biotechnol.* **2019**, *94*, 999–1007.
- (23) Van Renterghem, L.; Roelants, S. L. K. W.; Baccile, N.; Uyttersprot, K.; Taelman, M. C.; Everaert, B.; Mincke, S.; Ledegen, S.; Debrouwer, S.; Scholtens, K.; et al. From Lab to Market: An Integrated Bioprocess Design Approach for New-to-Nature Biosurfactants Produced by *Starmerella Bombicola*. *Biotechnol. Bioeng.* **2018**, *115*, 1195–1206.
- (24) Roelants, S. L. K. W.; Ciesielska, K.; De Maeseneire, S. L.; Moens, H.; Everaert, B.; Verweire, S.; Denon, Q.; Vanlerberghe, B.; Van Bogaert, I. N. A.; Van der Meeren, P.; et al. Towards the Industrialization of New Biosurfactants: Biotechnological Opportunities for the Lactone Esterase Gene from *Starmerella Bombicola*. *Biotechnol. Bioeng.* **2016**, *113*, 550–559.
- (25) Lodens, S.; Graeve, M. De; Roelants, S. L. K. W.; Maeseneire, S. L. De; Soetaert, W. Transformation of an Exotic Yeast Species into a Platform Organism: A Case Study for Engineering Glycolipid Production in the Yeast *Starmerella Bombicola*. *Methods Mol. Biol.* **2018**, *1772*, 95–123.
- (26) Van Bogaert, I. N. A.; Buyst, D.; Martins, J. C.; Roelants, S. L. K. W.; Soetaert, W. K. Synthesis of Bolaform Biosurfactants by an Engineered *Starmerella Bombicola* Yeast. *Biotechnol. Bioeng.* **2016**, *113*, 2644–2651.
- (27) Woltman, S. J.; Jay, G. D.; Crawford, G. P. Liquid-Crystal Materials Find a New Order in Biomedical Applications. *Nat. Mater.* **2007**, *6*, 929–938.
- (28) Dozov, I.; Paineau, E.; Davidson, P.; Antonova, K.; Baravian, C.; Bihannic, I.; Michot, L. J. Electric-Field-Induced Perfect Anti-Nematic Order in Isotropic Aqueous Suspensions of a Natural Beidellite Clay. *J. Phys. Chem. B* **2011**, *115*, 7751–7765.
- (29) Kleman, M.; Lavrentovich, O. *Soft Matter Physics: An Introduction*; Springer Science & Business Media, 2007.

- (30) Friedel, G.; Grandjean, F. Observations Géométriques Sur Les Liquides à Coniques Focales. *Bull. Minéralogie* **1910**, *33*, 409–465.
- (31) Fournier, J. B.; Durand, G. Focal Conic Faceting in Smectic-A Liquid Crystals. *J. Phys. II* **1991**, *1*, 845–870.
- (32) Halaby Macary, M.; Damême, G.; Gibek, A.; Dubuffet, V.; Dupuy, B.; Picart, J.; Dimeni, R. F.; Meyer, C. Optical Microscopy Observations and Construction of Dupin Cyclides at the Isotropic/Smectic A Phase Transition. *Materials (Basel)*. **2021**, *14*.
- (33) Saupe, A.; Boonbrahm, P.; Yu, L. Biaxial Nematic Phases in Amphiphilic Systems. *J. Chim. Phys.-Chim. Biol.* **1983**, *80*, 7–13.
- (34) Baccile, N.; Babonneau, F.; Jestin, J.; Pehau-Arnaudet, G.; Van Bogaert, I.; Péhau-Arnaudet, G.; Van Bogaert, I.; Pehau-Arnaudet, G.; Van Bogaert, I. Unusual, PH-Induced, Self-Assembly of Sophorolipid Biosurfactants. *ACS Nano* **2012**, *6*, 4763–4776.
- (35) Baccile, N.; Pedersen, J. S.; Pehau-Arnaudet, G.; Van Bogaert, I. N. a. Surface Charge of Acidic Sophorolipid Micelles: Effect of Base and Time. *Soft Matter* **2013**, *9*, 4911–4922.
- (36) Baccile, N.; Selmane, M.; Le Griel, P.; Prévost, S.; Perez, J.; Stevens, C. V.; Delbeke, E.; Zibek, S.; Guenther, M.; Soetaert, W.; et al. PH-Driven Self-Assembly of Acidic Microbial Glycolipids. *Langmuir* **2016**, *32*, 6343–6359.
- (37) Baccile, N.; Cuvier, A.-S.; Prévost, S.; Stevens, C. V.; Delbeke, E.; Berton, J.; Soetaert, W.; Van Bogaert, I. N. A.; Roelants, S. Self-Assembly Mechanism of PH-Responsive Glycolipids: Micelles, Fibers, Vesicles, and Bilayers. *Langmuir* **2016**, *32*, 10881–10894.
- (38) Davis, E. J.; Goodby, J. W. *Handbook of Liquid Crystals, Vol. 6*, 2nd Editio.; Al., J. W. G. et, Ed.; Wiley-VCH Verlag, 2014.
- (39) Oswald, P.; Pieranski, P. *Smectic and Columnar Liquid Crystals: Concepts and Physical Properties Illustrated by Experiments*; CRC Press, 2005.
- (40) Seddon, J. M. Structure of the Inverted Hexagonal (HII) Phase, and Non-Lamellar Phase Transitions of Lipids. *BBA - Rev. Biomembr.* **1990**, *1031*, 1–69.
- (41) Hirst, L. S. *Handbook of Liquid Crystals*; WILEY-VCH Verlag, 2014.
- (42) Diat, O.; Roux, D.; Nallet, F. Effects of Shear on a Lyotropic Lamellar Phase. *J. Phys. II Fr.* **1993**, *3*, 1427–1452.
- (43) Mitchell, D. J.; Tiddy, G. J. T.; Waring, L.; Bostock, T.; McDonald, M. P. Phase Behaviour of Polyoxyethylene Surfactants with Water. Mesophase Structures and Partial Miscibility (Cloud Points). *J. Chem. Soc. Faraday Trans. 1 Phys. Chem. Condens. Phases* **1983**, *79*, 975–1000.
- (44) Varade, D.; Aramaki, K.; Stubenrauch, C. Phase Diagrams of Water–Alkyltrimethylammonium Bromide Systems. *Colloids Surfaces A Physicochem. Eng. Asp.* **2008**, *315*, 205–209.
- (45) Kékicheff, P.; Grabielle-Madelmont, C.; Ollivon, M. Phase Diagram of Sodium Dodecyl Sulfate-Water System: 1. A Calorimetric Study. *J. Colloid Interface Sci.* **1989**, *131*, 112–132.
- (46) Smith, G. S.; Safinya, C. R.; Roux, D.; Clark, N. A. X-Ray Study Of Freely Suspended Films Of A Multilamellar Lipid System. *Mol. Cryst. Liq. Cryst.* **1987**, *144*, 235–255.
- (47) Baccile, N.; Le Griel, P.; Prévost, S.; Everaert, B.; Van Bogaert, I. N. A.; Roelants, S.; Soetaert, W. Glucosomes: Glycosylated Vesicle-in-Vesicle Aggregates in Water from PH-Responsive Microbial Glycolipid. *ChemistryOpen* **2017**, *6*, 526–533.
- (48) Imura, T.; Ohta, N.; Inoue, K.; Yagi, N.; Negishi, H.; Yanagishita, H.; Kitamoto, D. Naturally Engineered Glycolipid Biosurfactants Leading to Distinctive Self-Assembled

- Structures. *Chem. - A Eur. J.* **2006**, *12*, 2434–2440.
- (49) Israelachvili, J. N.; Mitchell, D. J.; Ninham, B. W. Theory of Self-Assembly of Hydrocarbon Amphiphiles into Micelles and Bilayers. *J. Chem. Soc. Faraday Trans. 2* **1976**, *72*, 1525.
- (50) Blackmore, E. S.; Tiddy, G. J. T. Phase Behaviour and Lyotropic Liquid Crystals in Cationic Surfactant-Water Systems. *J. Chem. Soc. Faraday Trans. 2 Mol. Chem. Phys.* **1988**, *2*, 1115–1127.
- (51) Imura, T.; Ikeda, S.; Aburai, K.; Taira, T.; Kitamoto, D. Interdigitated Lamella and Bicontinuous Cubic Phases Formation from Natural Cyclic Surfactin and Its Linear Derivative. *J. Oleo Sci.* **2013**, *62*, 499–503.
- (52) Dahrazma, B.; Mulligan, C. N.; Nieh, M. P. Effects of Additives on the Structure of Rhamnolipid (Biosurfactant): A Small-Angle Neutron Scattering (SANS) Study. *J. Colloid Interface Sci.* **2008**, *319*, 590–593.
- (53) Nagarajan, R. Self-Assembly of Bola Amphiphiles. *Chem. Eng. Commun.* **1987**, *55*, 251–273.
- (54) Baccile, N.; Renterghem, L. Van; Griel, P. Le; Ducouret, G.; Brennich, M.; Cristiglio, V.; Roelants, S. L. K. W.; Soetaert, W. Bio-Based Glyco-Bolaamphiphile Forms a Temperature-Responsive Hydrogel with Tunable Elastic Properties. *Soft Matter* **2018**, *14*, 7859–7872.
- (55) Baccile, N.; Delbeke, E. I. P.; Brennich, M.; Seyrig, C.; Everaert, J.; Roelants, S. L. K. W.; Soetaert, W.; Bogaert, I. N. A. Van; Geem, K. M. Van; Stevens, C. V. Asymmetrical, Symmetrical, Divalent and Y-Shaped (Bola)Amphiphiles: The Relationship between Molecular Structure and Self-Assembly in Amino Derivatives of Sophorolipid Biosurfactants. *J. Phys. Chem. B* **2019**, *123*, 3841–3858.
- (56) Peters, K. C.; Mekala, S.; Gross, R. A.; Singer, K. D. Cooperative Self-Assembly of Helical Exciton-Coupled Biosurfactant-Functionalized Porphyrin Chromophores. *ACS Appl. Bio Mater.* **2019**, *2*, 1703–1713.
- (57) Peters, K. C.; Mekala, S.; Gross, R. A.; Singer, K. D. Chiral Inversion and Enhanced Cooperative Self-Assembly of Biosurfactant-Functionalized Porphyrin Chromophores. *J. Mater. Chem. C* **2020**, *8*, 4675–4679.
- (58) Meister, A.; Blume, A. Self-Assembly of Bipolar Amphiphiles. *Curr. Opin. Colloid Interface Sci.* **2007**, *12*, 138–147.
- (59) Poirier, A.; Griel, P. Le; Zinn, T.; Pernot, P.; Roelants, S.; Soetaert, W.; Baccile, N. Energy Landscape of Sugar Conformation Controls the Sol-to-Gel Transition in Self-Assembled Bola Glycolipid Hydrogels. *Submitted* **2022**, <https://hal.archives-ouvertes.fr/hal-03576369v1>.
- (60) De Clercq, V.; Roelants, S. L. K. W.; Castelein, M. G.; De Maeseneire, S. L.; Soetaert, W. K. Elucidation of the Natural Function of Sophorolipids Produced by *Starmerella Bombicola*. *J. Fungi* **2021**, *7*, 917.

